

B_s PHYSICS AT CDF AND DØ

Harold G. Evans

Physics Department, Indiana University, Bloomington, IN, 47405, USA
(for the CDF and DØ Collaborations)

Abstract

Run II at the Tevatron has seen an explosion of results related to the B_s meson, ranging from tests of QCD models, to probes of electro-weak symmetry breaking, to direct searches for new physics effects. I will briefly summarize the CDF and DØ B_s -physics programs, describing the suitability of the detectors for doing this kind of physics, and pointing out how our knowledge of important quantities has improved through Run II measurements.

1 Introduction

Who would have thought it would be so fruitful?¹ In the past two years, CDF and D0 have produced over 35 separate results using B_s mesons. This represents the largest component of the Tevatron B-physics program, and, indeed, puts the B_s meson in the position of being the second-most prolific particle, in terms of physics output, in the Tevatron zoo – right after the top quark. This handy hadron has been used to study such diverse topics as QCD model building, physics beyond the Standard Model, the electro-weak symmetry breaking mechanism, and CP violation, to name just a few. In all of these areas, recent B_s results have sharpened our knowledge of the Standard Model and its weaknesses substantially.

Success comes at a price though – at least for conference audiences. The overwhelming number of results means that we cannot discuss any of their beautiful facets in detail; this article is already long enough. We will therefore concentrate on emphasizing the breadth of physics issues addressed by studies of the B_s meson, and will show how our understanding of these issues has improved since data from Run II at the Tevatron has been analyzed.

Obviously, this represents a snapshot of the Tevatron B_s -physics program, taken with up to 1.3 fb^{-1} of data. The Fermilab Tevatron accelerator continues to deliver proton-antiproton collisions to CDF and D0 at a furious pace. At the time of the conference each experiment had recorded over 2 fb^{-1} of data, with more rolling in every day. The final section of these proceedings will then be devoted to a brief discussion of what we plan to do with the bounty of B_s mesons that will come with this additional data.

2 The B_s at CDF and D0

Before we embark upon a description of results, it's instructive to examine the capabilities of the Tevatron collider experiments in areas important to the study of B_s mesons. Both CDF ¹⁾ and D0 ²⁾ are well suited to take advantage of the large number of B_s mesons produced in proton-antiproton collisions at the

¹ In fact, many people have recognized the utility of the B_s meson for years now, but it did come as some surprise to the CDF and D0 B-Physics communities that B_s analyses have proven to be such a dominant component of the Tevatron B-Physics program.

Tevatron. The B_s production rate within the CDF and D0 detector acceptance is around 600 Hz, at luminosities of $2 \times 10^{32} \text{ cm}^{-2}\text{s}^{-1}$. This can be compared to around 1 Hz at the B-factories, when they run at the $\Upsilon(5S)$ resonance; and 5000 Hz at the upcoming LHCb experiment. Thus the Tevatron is the only facility where B_s mesons are produced currently in any large numbers.

This large B_s production rate, however, is dwarfed by the rate of $p\bar{p}$ bunch crossings (1.7 MHz) meaning that triggers are critical to the B-physics program at the Tevatron. Both CDF and D0 use three-level trigger systems and rely heavily (almost exclusively in D0's case) on single or di-lepton signals to collect samples of B_s mesons. D0 makes use of its excellent muon detectors to construct low p_T threshold single- and di-muon triggers without resorting to muon impact parameter cuts, which bias decay length distributions, except at the highest Tevatron luminosities. CDF uses both electrons and muons for B-physics triggers, but applies impact parameter cuts to most single-lepton triggers.

Because the CDF trigger system is capable of accepting events from its first level at a rate of up to 30 kHz (the corresponding D0 level-1 bandwidth limit is around 2 kHz), the CDF collaboration has been able to design triggers that select, at level-1, events with two tracks forming a vertex displaced from the primary $p\bar{p}$ interaction point. Such events are enriched with fully hadronic decays of B mesons, which allows CDF access to the wide range of important studies that can be done using these decay modes.

For many of the analyses discussed in this article the primary means of identifying B_s mesons is through their semileptonic decay: $B_s \rightarrow D_s^- \ell^+ \nu_\ell X$. This decay has a branching fraction of 7.9%³⁾, and its identification highlights many of the experimental challenges that face CDF and D0. To begin with, there is the issue of lepton identification. D0 has the advantage here because of their muon detectors, which extend to pseudo-rapidities ($\eta = -\ln[\tan(\theta/2)]$) between ± 2 , while CDF's muon system covers only $|\eta| < 1$. Additionally, the D0 muon system is shielded by 12–18 interaction lengths of material (a factor of around three more than CDF's) and includes toroidal magnets for local muon momentum measurements. Taken together, these reduce many muon background sources in D0 to a negligible level.

Identification of D_s meson decays, on the other hand, requires excellent tracking capabilities. The experiments use $\phi(K^+K^-)\pi^+$, $\bar{K}^{*0}(K^-\pi^+)K^+$,

$K_S^0(\pi^+\pi^-)K^+$, and $\pi^+\pi^-\pi^+$ decay modes of the D_s^+ (and charge conjugates) in a range of analyses. CDF has the edge here, mainly because of the larger volume of their tracking system (extending from radii of 1.5 – 137 cm, as compared to the D0 tracker, which spans 2.8 – 52 cm) and the larger number of space-point measurements it makes (normally more than 100 for CDF, but only ~ 20 for D0). This allows CDF to reconstruct multi-particle invariant masses with significantly better accuracy than D0, making combinatorial backgrounds less of a problem.

Finally, both detectors reconstruct displaced vertices with similar resolution, although CDF does a slightly better job because their tracking extends to lower radii². As we will see, resolution is particularly important in B_s -mixing analyses, where time structures on the order of 100 fs must be reconstructed. Both the CDF and D0 tracking systems are capable of this feat in the reconstruction of semileptonic B_s decays, having average resolutions in the 15-20 fs range. However, because of CDF's large fully hadronic B_s decay sample, they are also able to take advantage of the better vertexing resolution (< 10 fs) achievable in these types of decay.

Using these upgraded detectors, both experiments have been able to accumulate B_s meson data samples that contain orders of magnitude more events than have previously been observed at LEP or Run I at the Tevatron (1992–1996). Now let's look at what we've done with this harvest.

3 Properties of B_s Mesons

Knowledge of the basic properties of the B_s meson – how it is produced, how massive it is, how long it lives, how it decays – is the foundation upon which we build all subsequent studies using the particle. Accurate measurements of these quantities are thus essential for the tests of the Standard Model, and the searches for its extensions, described later. However, B_s property determinations are also useful in themselves as tests of our ability to use QCD, whether through models or by lattice calculations. Measurements made by CDF and D0 since the start of Run II have substantially increased our knowledge in the full range of this area.

² Note that D0 added a *Layer-0* silicon detector at a radius of 1.7 cm in June, 2006. Results using this new detector were not yet available for this conference though.

3.1 Production Fraction

Let's start with production. A major question here concerns whether the fragmentation of quark-antiquark pairs into heavy flavor hadrons is governed by universal functions independent of the type of collisions producing the quarks. CDF has made preliminary measurements of the relative fragmentation fractions of B hadrons in $p\bar{p}$ collisions. Their preliminary measurement of the B_s fraction relative to that of B_u and B_d uses $B_s \rightarrow \ell^- D_s^+ X$ decays in 0.36 fb^{-1} of data:

$$\frac{f_s}{f_u + f_d} = 0.160 \pm 0.005 \text{ (stat)} \begin{matrix} +0.011 \\ -0.010 \end{matrix} \text{ (syst)} \begin{matrix} +0.057 \\ -0.034 \end{matrix} \text{ (BR)},$$

where the last error reflects the uncertainty on the $D_s^+ \rightarrow \phi \pi^+$ branching ratio. When corrected for f_u and f_d , their measurement, $f_s = (12.7 \pm 3.8)\%$ is consistent with, but slightly higher than the LEP average of $(10.4 \pm 0.9)\%$ ⁴⁾, indicating that no large differences in fragmentation between e^+e^- and $p\bar{p}$ are likely.

3.2 Mass and Lifetime

Mass and lifetime are also important properties of the B_s meson, and Run II results have dramatically improved our knowledge of them. Before the start of Run II, the B_s mass world average of $5369.6 \pm 2.4 \text{ MeV}$ ⁵⁾ was dominated by 32 $B_s \rightarrow J/\psi \phi$ candidates reconstructed by CDF. Using 0.22 fb^{-1} of data from Run II, corresponding to 185 candidate decays, CDF has improved this measurement by almost a factor of three to $5366.01 \pm 0.73 \pm 0.33 \text{ MeV}$ ⁶⁾. On the lifetime side, both CDF and D0 have contributed to a factor of two improvement in the accuracy of the mean B_s lifetime measurement since the start of Run II: from $\tau(B_s) = 1.461 \pm 0.057 \text{ ps}$ in 2003 ⁵⁾ to $\tau(B_s) = 1.451 \begin{matrix} +0.029 \\ -0.028 \end{matrix} \text{ ps}$ in 2006 ⁴⁾. Although each experiment has measured the B_s lifetime in several different modes, which contain different mixtures of CP -even and CP -odd states (as discussed later in this article), the most precise measurement, $\tau(B_s) = 1.398 \pm 0.044 \begin{matrix} +0.029 \\ -0.028 \end{matrix} \text{ ps}$, currently comes from D0's analysis of $B_s \rightarrow D_s \mu X$ decays in 0.40 fb^{-1} of data ⁷⁾.

Using the new average B_s lifetime, we find agreement with predictions of the lifetime ratio $\tau(B_s)/\tau(B_d)$, calculated using heavy quark effective theory, at the 2.3-sigma level:

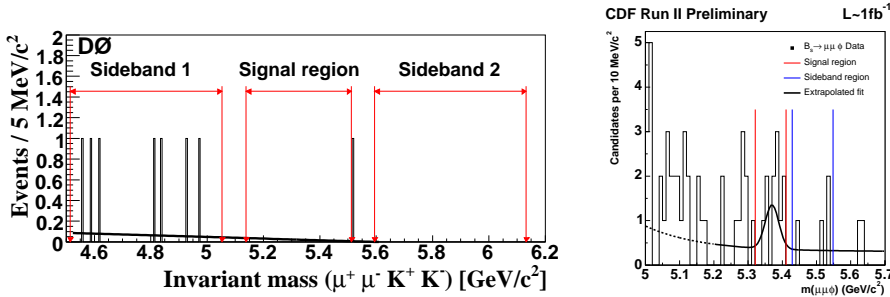


Figure 1: The $\mu^+\mu^-\phi$ invariant mass distribution observed by D0 (left) and CDF (right).

$$\begin{array}{ll} \text{Experiment} & 0.950 \pm 0.019 \text{ }^4) \\ \text{NLO Theory} & 1.00 \pm 0.01 \text{ }^8). \end{array}$$

Note especially that the accuracy of the experimental measurements is now approaching that of the theoretical predictions for this ratio.

3.3 Hadronic Branching Ratios

Making use of their 2-track trigger, CDF has been able to accumulate an unprecedented sample of fully hadronic B_s decays. This allows them to make measurements, often for the first time ever, of various rare mode branching ratios as shown in tab. 1. These measurements provide valuable tests of QCD models, particularly of the applicability of SU(3) quark symmetries. With more statistics, some of them will also allow sensitive tests of CP violation: the angle γ/ϕ_3 of the CKM triangle from studies of $B_s \rightarrow h^+h^-$, and probes of CP -even vs. CP -odd contributions using the $\psi(2S)\phi$ and $\phi\phi$ modes.

Measurements of orbitally excited B_s mesons have also been made by CDF and D0. However, these are discussed in another contribution to these proceedings ¹⁸⁾.

4 Flavor Changing Neutral Current Decays

Decays of B hadrons governed by flavor changing neutral currents provide sensitive probes for new physics because these decays are highly suppressed in

Table 1: *Hadronic B_s branching ratio measurements compared to theoretical expectations.*

Mode	Lumi	Signal	Measurement [Prediction]
$\frac{\mathcal{B}(B_s \rightarrow D_s^- \pi^+)}{\mathcal{B}(B^0 \rightarrow D^- \pi^+)}$	0.355 fb ⁻¹	494 ± 28	1.13 ± 0.08 ± 0.23 ⁹⁾ [1.05 ± 0.24] ¹⁰⁾
$\frac{\mathcal{B}(B_s \rightarrow D_s^- \pi^+ \pi^+ \pi^-)}{\mathcal{B}(B^0 \rightarrow D^- \pi^+ \pi^+ \pi^-)}$	0.355 fb ⁻¹	309 ± 26	1.05 ± 0.10 ± 0.22 ⁹⁾
$\mathcal{B}(B_s \rightarrow K^+ K^-) (\times 10^6)$	1.0 fb ⁻¹	1307 ± 64	24.4 ± 1.4 ± 4.6 (prelim) [20 ± 9] ¹¹⁾ [35 ⁺⁷³ ₋₂₀] ¹²⁾
$\mathcal{B}(B_s \rightarrow K^- \pi^+) (\times 10^6)$	1.0 fb ⁻¹	230 ± 38	5.00 ± 0.75 ± 1.00 (prelim) [4.9] ¹³⁾
$\mathcal{B}(B_s \rightarrow \pi^+ \pi^-) (\times 10^6)$	1.0 fb ⁻¹	26 ± 21	<1.36 at 90% CL (prelim)
$\frac{\mathcal{B}(B_s \rightarrow \psi(2S) \phi)}{\mathcal{B}(B_s \rightarrow J/\psi \phi)}$	0.36 fb ⁻¹	32.5 ± 6.5	0.52 ± 0.13 ± 0.07 ¹⁴⁾ [0.54 ± 0.06] ¹⁵⁾
$\mathcal{B}(B_s \rightarrow \phi \phi) (\times 10^6)$	0.18 fb ⁻¹	7.3 ± 2.9	14 ⁺⁶ ₋₅ ± 6 ¹⁶⁾ [10 – 37] ¹⁷⁾

the Standard Model, proceeding through loop diagrams. In many models of physics beyond the Standard Model, however, these types of decays can be enhanced in some regions of model parameter space. For example, $\mathcal{B}(B_s \rightarrow \mu^+ \mu^-)$ is proportional to $\tan^6 \beta$ ³ in the minimal supersymmetric standard model ¹⁹⁾.

CDF and D0 have searched for flavor changing neutral currents in decays of B_s mesons to $\mu^+ \mu^-$ and in the decay $B_s \rightarrow \mu^+ \mu^- \phi$. Results are shown in tab. 2. The new limits on $\mathcal{B}(B_s \rightarrow \mu^+ \mu^-)$ represent more than an order of magnitude improvement over those available before Run II data was analyzed ⁵⁾ and are now only a factor of 30 from the Standard Model prediction. In the decay $B_s \rightarrow \mu^+ \mu^- \phi$, studied for the first time with Run II data, CDF sees a 2.3-sigma excess of events, as shown in fig. 1 – so observation of this mode could be just around the corner!

³ β is the ratio of the vacuum expectation value of the two Higgs doublets.

Table 2: *Experimental limits and standard model predictions for flavor changing neutral current B meson decays.*

Mode	Exp.	Lumi	Evs	Bgrd	95% CL Limit
$B_s \rightarrow \mu^+ \mu^-$	D0	0.30 fb^{-1}	4	4.3 ± 1.2	$< 4.0 \times 10^{-7}$ (prelim) ^a
	CDF	0.78 fb^{-1}	1	1.27 ± 0.37	$< 1.0 \times 10^{-7}$ (prelim)
	Pred.				$(3.42 \pm 0.54) \times 10^{-9}$ 20)
$B_s \rightarrow \mu^+ \mu^- \phi$	D0	0.45 fb^{-1}	0	1.6 ± 0.4	$< 4.1 \times 10^{-6}$ 21)
	CDF	0.92 fb^{-1}	11	3.5 ± 1.5	$< 2.4 \times 10^{-6}$ (prelim)
	Pred.				$(1.6 \pm 0.5) \times 10^{-6}$ 22)

^aShortly after the end of this conference D0 announced a new, preliminary $B_s \rightarrow \mu^+ \mu^-$ limit of 9.3×10^{-8} at the 95% CL, using 2 fb^{-1} of data.

5 Mixing and CP Violation

The phenomenon of mixing between neutral mesons and anti-mesons provides a very sensitive probe of the mechanism of electro-weak symmetry breaking. This sensitivity is due to the fact that flavor structure in the Standard Model, in particular the difference between quark weak and mass eigenstates, arises through Yukawa couplings of fermions to the Higgs boson²³). Thus, time evolution in the neutral B systems is governed by the Schrödinger equation:

$$i \frac{d}{dt} \begin{pmatrix} |B(t)\rangle \\ |\bar{B}(t)\rangle \end{pmatrix} = \begin{pmatrix} M - \frac{i\Gamma}{2} & M_{12} - \frac{i\Gamma_{12}}{2} \\ M_{12}^* - \frac{i\Gamma_{12}^*}{2} & M - \frac{i\Gamma}{2} \end{pmatrix} \begin{pmatrix} |B(t)\rangle \\ |\bar{B}(t)\rangle \end{pmatrix} \quad (1)$$

and the eigenstates of the mass matrix, B_L, B_H , are different than the weak eigenstates, B, \bar{B} , which oscillate between each other. These oscillations can be described by three parameters: $|M_{12}|$, $|\Gamma_{12}|$, and the CP -violating phase, $\phi = \arg(-M_{12}/\Gamma_{12})$, which are related to physical observables:

$$\begin{aligned} \Delta m &= M_H - M_L && \sim 2|M_{12}| \\ \Delta\Gamma &= \Gamma_L - \Gamma_H && = \Delta\Gamma_{CP} \cos\phi \\ \Delta\Gamma_{CP} &= \Gamma_{CP-even} - \Gamma_{CP-odd} && \sim 2|\Gamma_{12}| \end{aligned} \quad (2)$$

In the B_s system, a measurement of the mass difference, Δm_s , which also gives the frequency of oscillations between particle and anti-particle states, allows the determination of the CKM matrix element V_{ts} . Although important

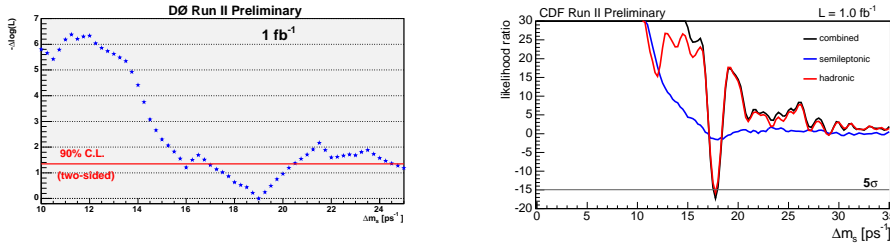


Figure 2: Likelihood scans of the $D0$ (left) and CDF (right) combined oscillation samples vs. Δm_s .

as parameters of the Standard Model, Δm_s and V_{ts} are most useful in constraining new physics when used in conjunction the B_d oscillation frequency via:

$$\frac{\Delta m_d}{\Delta m_s} = \frac{M(B_d)}{M(B_s)} \xi \left| \frac{V_{td}}{V_{ts}} \right|^2 \quad \xi = \frac{f_{B_d}^2 B_{B_d}}{f_{B_s}^2 B_{B_s}} \quad (3)$$

The ratio of Δm_d to Δm_s gives a more precise determination of V_{td} , related to one of the sides of the unitarity triangle²³⁾, because the theoretical uncertainty on ξ is much less than that on the individual lattice calculations of the B meson decay constants (f) and bag parameters (B)²⁴⁾.

The other B_s mixing observables are also important in searches for new physics. The ratio $\Delta\Gamma_s/\Delta m_s$ is a function of QCD parameters only, and thus provides a measurement in this system that is independent of new physics. The CP -violating phase, ϕ_s , however, is expected to be tiny in the Standard Model, $\sim 0.25^\circ$ ²⁵⁾. Theories of physics beyond the Standard Model, however, often include other sources of CP -violation than the single Standard Model phase, and can thus yield large predictions for ϕ_s .

5.1 B_s Oscillations

Spring 2006 was a watershed period in the study for B_s oscillations. After nearly two decades of searching for a B_s oscillations signal by many experimental groups, D0 was able to set the first two-sided bound on the parameter Δm_s by a single experiment²⁶⁾. CDF followed quickly thereafter with three-sigma evidence for B_s oscillations²⁷⁾.

The current status of B_s mixing measurements is shown in fig. 2 where a preliminary combination of D0 results is presented as well as the final CDF observation ²⁸⁾, which is now significantly more than a 5-sigma effect. Numerically, the results are:

$$\begin{array}{ll} \text{D0 (1 fb}^{-1}\text{)} & 17 < \Delta m_s < 21 \text{ ps}^{-1} \quad (90\% \text{ CL}) \\ \text{CDF (1 fb}^{-1}\text{)} & 17.77 \pm 0.10 \pm 0.07 \text{ ps}^{-1}. \end{array}$$

Some details of the analyses are presented in tab. 3, including the B_s decay modes used; sample sizes; the quality of the flavor taggers used to distinguish events where a B_s oscillated to a \bar{B}_s before decaying and vice-versa⁴; and the sensitivity of the analysis, defined as the expected limit in the absence of any signal. For reference, information about the previously most sensitive single channel – ALEPH’s fully hadronic signal ⁵⁾ – is also included.

CDF uses their measurement of Δm_s to derive a value for the ratio of CKM matrix elements:

$$\left| \frac{V_{td}}{V_{ts}} \right| = 0.2060 \pm 0.0007(\text{exp}) \begin{array}{l} +0.0081 \\ -0.0060 \end{array}(\text{theory}).$$

The accuracy on this quantity is now completely dominated by the uncertainty of the ratio of B_s and B_d decay constants and bag parameters, ξ , from lattice calculations ²⁴⁾.

BaBar and Belle have also recently measured $|V_{td}/V_{ts}|$ using B_d decays to $\rho\gamma$ and $K^*\gamma$ ³⁵⁾. The average of their results, $0.200 \pm 0.016(\text{exp}) \begin{array}{l} +0.016 \\ -0.015 \end{array}(\text{theory})$, is consistent with the CDF measurement but of significantly lower sensitivity. Interestingly, however, the B-factory measurement is still dominated by experimental uncertainties, while the theoretical error on its value is only slightly larger than that on CDF’s measurement. The addition of enough data to bring the experimental uncertainty on the B-factory measurements below that from theory will make this measurement competitive with, and complimentary to, the matrix element ratio measurements from the Tevatron.

Table 3: Details of the $D0$ and CDF B_s oscillation analyses. Also shown are comparable numbers for the previously most sensitive analysis from ALEPH.

Mode	Sample	Average εD^2		Sensitivity
		OST	SST	
ALEPH fully hadronic	28.5	27%		13.6 ps ⁻¹
D0 Semileptonic $\ell D_s; D_s \rightarrow \phi \pi^-, K^{*0} K^-, K_S^0 K^-$	43,000	2.48%		16.5 ps ⁻¹
CDF Semileptonic $\ell D_s; D_s \rightarrow \phi \pi^-, K^{*0} K^-, 3\pi^\pm$	61,500	1.8%	4.8%	19.3 ps ⁻¹
CDF Hadronic $D_s \pi^+, D_s 3\pi^\pm; D_s \rightarrow \phi \pi^-, K^{*0} K^-, 3\pi^\pm$	8,700	1.8%	3.7%	30.7 ps ⁻¹

5.2 B_s Width Difference and CP -violating Phase

Not content with measuring only the mass difference part of B_s mixing, intrepid analysts also made major progress on the other parameters, $\Delta\Gamma_s$ and ϕ_s , in the last year. These quantities can be accessed by combining information from several sources:

1. $B_s \rightarrow J/\psi \phi$: the time evolution, mass and angular distributions in $B_s \rightarrow J/\psi \phi$ decays;
2. τ_{fs} : lifetimes of flavor-specific B_s decays, for example semi-leptonic decays, which contain an equal mixture of CP -even and CP -odd components;
3. $A_{SL}^{\mu\mu}$: charge asymmetries in like-sign dimuon production;
4. A_{SL}^z : charge asymmetries in $B_s \rightarrow \mu^\pm D_s^\mp$ decays;
5. $\tau_{even}, \mathcal{B}_{even}$: lifetimes and branching ratios of CP -specific B_s decays, such as $B_s \rightarrow K^+ K^-$ and $B_s \rightarrow D_s^{(*)} D_s^{(*)}$.

⁴ This quality is defined as εD^2 , the efficiency of the tagger times the dilution squared (where the dilution, $D = 1 - 2P_{mis-tag}$, with $P_{mis-tag}$ being the probability to incorrectly tag the event). It is measured using information about the *other* B hadron in the event (OST) or using particles associated with the B_s meson (SST)

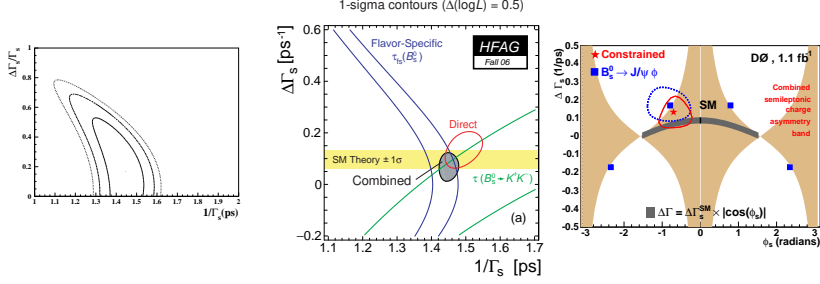


Figure 3: Plots of the world average values of $\Delta\Gamma_s$ vs. $1/\Gamma_s$ from winter 2003⁵⁾ (left) and the end of 2006⁴⁾ (middle). Also show is the combination³⁴⁾ of $D0$ measurements of $\Delta\Gamma_s$ vs ϕ_s (right).

In the past, analyses centered on the extraction of $\Delta\Gamma_s$ using the first two methods described above. The state-of-the-art in early 2003 can be seen in the left-most plot of fig. 3, which shows that no statistically significant extraction of the value of $\Delta\Gamma_s$ could be made before Run II results were available.

This has changed dramatically in the past year, with a flurry of new results from $D0$ and CDF , which are summarized in tab. 4. Combining these results (with the exception of the $D0$ and CDF $B_s \rightarrow D_s^{(*)} D_s^{(*)}$ measurements where the assumption of CP -even state dominance is unproven) yields averages summarized in the center plot of fig. 3⁴⁾. Progress is clearly substantial, with a new world-average value of

$$\Delta\Gamma_s = 0.071_{-0.057}^{+0.053} \text{ ps}^{-1} \quad (-0.04 < \Delta\Gamma_s < +0.17) \text{ ps}^{-1} \quad (95\% \text{ CL}).$$

This measurement, favors a positive, non-zero value for $\Delta\Gamma_s$, and is in agreement with the Standard Model expectation of $0.088 \pm 0.017 \text{ ps}^{-1}$ ²⁵⁾.

Their large B_s data samples and multiple handles on mixing also allow $D0$ to perform a combination of their results³⁴⁾, shown in the right-hand plot of fig. 3, that is sensitive to ϕ_s . This combination results in a value of $\Delta\Gamma_s = 0.13 \pm 0.09 \text{ ps}^{-1}$, which is consistent with the world average; and finds:

$$\phi_s = -0.70_{-0.39}^{+0.47}$$

which is nearly 2-sigma away from $(4.2 \pm 1.4) \times 10^{-3}$ ²⁵⁾, the Standard Model prediction.

Table 4: A summary of recent analyses sensitive to $\Delta\Gamma_s$ and ϕ_s .

Tech.	Exp. Lumi Signal	Observables Measurement	Sens. to $\Delta\Gamma_s, \phi_s$
$B_s \rightarrow J/\psi\phi$	CDF ²⁹⁾ 0.355 fb ⁻¹ 203±15	$M(J/\psi\phi)$, proper time, 3 decay angles $\Delta\Gamma_s = 0.47^{+0.19}_{-0.24} \pm 0.01$ ps ⁻¹	fit for: $\Delta\Gamma_s, \tau_{fs}$ helicity amplitudes
$B_s \rightarrow J/\psi\phi$	D0 ³⁰⁾ 1.1 fb ⁻¹ 1039±45	$M(J/\psi\phi)$, proper time, 3 decay angles $\Delta\Gamma_s = 0.17 \pm 0.09$ ps ⁻¹ $\phi_s = -0.79 \pm 0.56$	fit for: $\Delta\Gamma_s, \phi_s, \tau_{fs}$ helicity amplitudes, strong phases
τ_{fs}	W.A. ⁴⁾	$\tau_{fs} = 1.440 \pm 0.036$ ps	τ_{fs} $= \frac{1}{\Gamma_s} \left[\frac{1 + (\Delta\Gamma_s/2\Gamma_s)^2}{1 - (\Delta\Gamma_s/2\Gamma_s)^2} \right]$
$A_{SL}^{\mu\mu}$	D0 ³¹⁾ 1.0 fb ⁻¹	$\frac{N(bb \rightarrow \mu^+\mu^+) - N(bb \rightarrow \mu^-\mu^-)}{N(bb \rightarrow \mu^+\mu^+) + N(bb \rightarrow \mu^-\mu^-)}$ $A_{SL}^{\mu\mu} = (-0.92 \pm 0.44 \pm 0.32)\%$	$A_{SL}^{\mu\mu} = A_{SL}^d + \frac{f_s Z_s}{f_d Z_d} A_{SL}^s$ $Z_q = \frac{1}{1 - (\Delta\Gamma_q/2\Gamma_q)^2}$ $-\frac{1}{1 + (\Delta m_q/\Gamma_q)^2}$
A_{SL}^s	D0 ³²⁾ 1.3 fb ⁻¹ 27,300±300	$\frac{N(\mu^+ D_s^-) - N(\mu^- D_s^+)}{N(\mu^+ D_s^-) + N(\mu^- D_s^+)}$ $A_{SL}^s = (1.23 \pm 0.97 \pm 0.17)\%$	A_{SL}^s $= \frac{1}{2} \frac{x_s^2 + y_s^2}{1 + x_s^2} \frac{\Delta\Gamma_s}{\Delta m_s} \tan \phi_s$
τ_{even}	CDF prelim 360 fb ⁻¹ 718±55	$\tau(B_s \rightarrow K^+ K^-)$ 1.53±0.18±0.02 ps	τ_{even} $\sim \frac{1}{\Gamma_s} \left[\frac{1}{1 + (\Delta\Gamma_{CP}/2\Gamma_s)} \right]$
\mathcal{B}_{even}	CDF prelim 360 fb ⁻¹ 718±55	$\mathcal{B}(B_s \rightarrow D_s^+ D_s^-)$ $= (1.3 \pm 0.6)\%$	$2\mathcal{B}_{even}$ $\sim \frac{\Delta\Gamma_{CP}}{\Gamma_s} \left[\frac{1}{1 + (\Delta\Gamma_{CP}/2\Gamma_s)} \right]$
\mathcal{B}_{even}	D0 ³³⁾ 1.3 fb ⁻¹ 718±55	$\mathcal{B}(B_s \rightarrow D_s^{(*)} D_s^{(*)})$ $= (3.9^{+1.9}_{-1.7} \pm 1.6 \pm 1.5)\%$	

5.3 Direct CP - violation

As a final note to this section on CP measurements using the B_s , CDF has taken the first steps toward measuring direct CP -violation in the B_s system using their preliminary $B_s \rightarrow K^- \pi^+$ measurement, discussed previously. In addition to measuring the branching ratio for this mode, they also determine its CP asymmetry:

$$A_{CP} \equiv \frac{|A(B_s^0 \rightarrow K^- \pi^+)|^2 - |A(\bar{B}_s^0 \rightarrow K^+ \pi^-)|^2}{|A(B_s^0 \rightarrow K^- \pi^+)|^2 + |A(\bar{B}_s^0 \rightarrow K^+ \pi^-)|^2} = 0.39 \pm 0.15 \pm 0.08,$$

which differs from zero by 2.5-sigma and is in good agreement with the Standard Model expectation of ~ 0.37 ³⁶).

6 Future Prospects and Conclusions

Looking back on the last few years, we can take pride in the good use to which the B_s meson has been put at the Tevatron in Run II. We have observed many decay modes of this particle for the first time and are zeroing in on an observation of the flavor changing neutral current in $B_s \rightarrow \mu^+ \mu^- \phi$ decays, while being only a factor of 30 away from the Standard Model prediction for $B_s \rightarrow \mu^+ \mu^-$. We have also made remarkable progress in our understanding of B_s mixing, with a first observation of its oscillation frequency after more than a decade of searching; and new sensitivity to the CP -violating phase in this system. However, we certainly do not plan to rest on our laurels.

The Tevatron is operating extremely well, delivering luminosity at a pace where we can expect a total Run II data sample of up to 8 fb^{-1} per experiment. In addition, both experiments are upgrading their capabilities, with D0's new Layer-0 silicon detector of particular importance to the B-physics program. Although the larger instantaneous luminosities seen by CDF and D0 will force the imposition of more restrictive triggers, significantly larger B_s data samples should be available in the next 1–2 years. As many of the measurements presented here remain statistics limited (a notable expectation is the extraction of V_{td} from Δm_d and Δm_s) this added data should allow a vibrant continuing program of measurements of rare decay modes and CP -violation in the B_s system.

You have, most certainly, not heard the last of the B_s meson at the Tevatron!

Acknowledgments

I would like to thank the D0 and CDF B-physics working group convenors, Brendan Casey, Cheng-Ju Lin, Manfred Paulini, and Andrzej Zieminski, for their help in preparing this presentation. My warmest gratitude also goes to the conference organizers for preparing such a fascinating program (not to mention the excellent food, drink, and skiing)!

References

1. D. Acosta, *et al.* (CDF), Phys. Rev. **D 71**, 032001 (2005); R. Blair, *et al.* (CDF), Fermilab-Pub-96/390-E (1996); C.S. Hill, *et al.*, Nucl. Instrum. and Methods **A 530**, 1 (2004); W. Ashmanskas, *et al.*, Nucl. Instrum. and Methods **A 518**, 532 (2004); S. Cabrera, *et al.*, Nucl. Instrum. and Methods **A 494**, 416 (2002).
2. V.M. Abazov, *et al.* (D0), Nucl. Instrum. and Methods **A 565**, 463 (2006).
3. W.-M. Yao, *et al.* (The Particle Data Group), Journal of Phys. **G 33**, 1 (2006).
4. The Heavy Flavor Averaging Group (end of 2006 results), <http://www.slac.stanford.edu/xorg/hfag/>.
5. The Heavy Flavor Averaging Group (PDG 2003 results), <http://www.slac.stanford.edu/xorg/hfag/>; K. Hagiwara, *et al.* (The Particle Data Group), Phys. Rev. **D 66**, 1 (2002).
6. D. Acosta, *et al.* (CDF), Phys. Rev. Lett. **96**, 202001 (2006).
7. V.M. Abazov, *et al.* (D0), Phys. Rev. Lett. **97**, 241801 (2006).
8. C. Tarantino, Eur. Phys. J. **C 33**, S895 (2004); Nucl. Phys. Proc. Suppl. **156**, 33 (2006).
9. D. Acosta, *et al.* (CDF), Phys. Rev. Lett. **98**, 061802 (2007).
10. P. Colangelo and R. Ferrandes, Phys. Lett. **B 627**, 77 (2005).

11. S. Descotes-Genon, J. Matias, and J. Virto, Phys. Rev. Lett. **97**, 061801 (2006); S. Baek, D. London, J. Matias, and J. Virto, JHEP **0612**, 019 (2006).
12. from QCD sum rules, implying large U-spin violation
A.J. Buras, *et al.*, Nucl. Phys. **B 697**, 133 (2004); A. Khodjamirian, T. Mannel, and M. Melcher, Phys. Rev. **D 68**, 114007 (2003).
13. A.R. Williamson and J. Zupan, Phys. Rev. **D 74**, 014003 (2006).
14. D. Acosta, *et al.* (CDF), Phys. Rev. Lett. **98**, 061802 (2007).
15. from $\mathcal{B}(B^0 \rightarrow \psi(2S)K^{*0}) / \mathcal{B}(B^0 \rightarrow J/\psi K^{*0})$.
16. D. Acosta, *et al.* (CDF), Phys. Rev. Lett. **95**, 031801 (2005).
17. Y.-H. Chen, *et al.*, Phys. Rev. **D 59**, 074003 (1999); X.Q. Li, G.R. Lu, and Y.D. Yang, Phys. Rev. **D 68**, 114015 (2003) [Erratum-ibid. **D 71**, 019902 (2005)].
18. T. Kuhr, these proceedings.
19. see, T. Blazek, S.F. King, and J.K. Parry, Phys. Lett. **B 589**, 39 (2004).
20. A.J. Buras, Phys. Lett. **B 566**, 115 (2003).
21. V.M. Abazov, *et al.* (D0), Phys. Rev. **D 74**, 031107 (2006).
22. C.Q. Geng and C.C. Liu, Journal of Phys. **G 29**, 1103 (2003).
23. see K. Anikeev, *et al.*, Fermilab-Pub-01/197 [[arXiv:hep-ph/0201071](https://arxiv.org/abs/hep-ph/0201071)].
24. M. Okamoto, Proc. Sci. LAT2005 , 013 (2005) [[arXiv:hep-lat/0510113](https://arxiv.org/abs/hep-lat/0510113)].
25. A. Lenz and U. Nierste, [arXiv:hep-ph/0612167](https://arxiv.org/abs/hep-ph/0612167).
26. V.M. Abazov, *et al.* (D0), Phys. Rev. Lett. **97**, 021802 (2006).
27. D. Acosta, *et al.* (CDF), Phys. Rev. Lett. **97**, 062003 (2006).
28. D. Acosta, *et al.* (CDF), Phys. Rev. Lett. **97**, 242003 (2006).
29. D. Acosta, *et al.* (CDF), Phys. Rev. Lett. **94**, 101803 (2005).

30. V.M. Abazov, *et al.* (D0), Phys. Rev. Lett. **98**, 121801 (2007).
31. V.M. Abazov, *et al.* (D0), Phys. Rev. **D 74**, 112002 (2006).
32. V.M. Abazov, *et al.* (D0), Phys. Rev. Lett. **98**, 151801 (2007).
33. V.M. Abazov, *et al.* (D0), [arXiv:hep-ex/0702049](https://arxiv.org/abs/hep-ex/0702049).
34. V.M. Abazov, *et al.* (D0), [arXiv:hep-ex/0702030](https://arxiv.org/abs/hep-ex/0702030).
35. S. Nishida, these proceedings.
36. H.J. Lipkin, Phys. Lett. **B 621**, 126 (2005).